Multi-Objective Optimization of Material Removal Rate and Surface Roughness in Ultrasonic Vibration-Assisted EDM Using NSGA-II, GPR, and AHP

Van Thanh Dinh
East Asia University of Technology, Trinh Van Bo Street, Hanoi City 12000, Vietnam
thanh.dinh@eaut.edu.vn

Thu Quy Le
National Research Institute of Mechanical Engineering, 04 Pham Van Dong, Ha Noi City 11309, Vietnam
quylt@narime.gov.vn

Thi Tam Do
Thai Nguyen University of Technology, 3/2 street, Tich Luong Ward, Thai Nguyen City 251750, Vietnam
dothitam@tnut.edu.vn

Ngoc Pi Vu
Thai Nguyen University of Technology, 3/2 street, Tich Luong Ward, Thai Nguyen City 251750, Vietnam
vungocpi@tnut.edu.vn

Thi Phuong Thao Tran
Thai Nguyen University of Technology, 3/2 street, Tich Luong Ward, Thai Nguyen City 251750, Vietnam
tranphuongthao@tnut.edu.vn (corresponding author)

Received: 9 April 2025 | Revised: 25 May 2025 | Accepted: 1 June 2025

 DOI: https://doi.org/10.48084/etasr.11380

ABSTRACT

Ultrasonic Vibration-Assisted Electrical Discharge Machining (UV-EDM) constitutes a promising technique for improving machining efficiency and surface quality, particularly when working with difficult-to-machine materials. This study presents a comprehensive multi-objective optimization approach for UV-EDM applied to 90CrSi steel, aiming to maximize the Material Removal Rate (MRR) while minimizing Surface Roughness (Ra). The experimental data were collected under varying process parameters, including the peak current, pulse-on time, and ultrasonic vibration amplitude. A Gaussian Process Regression (GPR) model was developed to accurately predict MRR and R_a. These predictive models were then integrated into the Non-Dominated Sorting Genetic Algorithm II (NSGA-II) to perform Pareto-based optimization. Additionally, the Analytic Hierarchy Process (AHP) was employed to rank the Pareto-optimal solutions based on decision-makers' preferences. The results demonstrate the effectiveness of combining GPR and NSGA-II for modeling and optimizing UV-EDM, while the use of AHP enables a rational selection of optimal machining conditions. This hybrid methodology offers valuable insights into enhancing productivity and surface integrity in precision machining applications.

Keywords-ultrasonic vibration assisted EDM; material removal rate; surface roughness; NSGA-II; Gaussian process regression; AHP; multi objective optimization

I. INTRODUCTION

Electrical Discharge Machining (EDM) is an effective technique for machining hard-to-cut materials and complex geometries. However, traditional EDM processes face notable challenges, including low MRR, excessive tool wear, and poor surface finish. UV-EDM has emerged as a promising hybrid technique to overcome these limitations by enhancing debris evacuation, stabilizing discharges, and reducing tool wear [1, 2].

The role of ultrasonic vibrations applied to either the tool, workpiece, or dielectric fluid has been investigated. Authors in [3] demonstrated that applying longitudinal/torsional vibrations significantly reduces taper formation and enhances debris motion in deep-hole EDM. Similarly, the mechanisms of debris removal in UV-EDM drilling have been explored, with emphasis placed on the impact of improved flushing on machining stability [1]. A novel approach using longitudinal torsional vibration electrodes was introduced to improve MRR and hole quality [4]. These studies highlight the potential of UV-EDM in improving process performance, particularly for micro-features.

Surface integrity is another critical concern in EDM. It has been shown that circular or multidimensional ultrasonic vibrations yield smoother surfaces and reduced recast layer thickness in micro-EDM applications [5]. Several studies have also explored the use of powder-mixed dielectric fluids in UV-EDM, aiming to further improve machining efficiency and stability. These modifications have been shown to affect spark behavior, debris removal, and overall discharge consistency. In parallel, the influence of cavitation effects and thermodynamic phenomena in UV-EDM has been addressed, supporting the need for more refined modeling and control strategies [6].

Despite recent advances, most previous works have focused on empirical evaluations rather than intelligent optimization frameworks. In response, multi-objective optimization techniques, such as NSGA-II, as well as hybrid models with machine learning (e.g. GPR), have attracted increasing interest. However, only a limited number of studies integrate these approaches with UV-EDM. The combined use of finite element modeling and experimental validation has been employed to investigate the tool vibration effects, whereas fuzzy logic has been utilized to support parameter selection in UV-EDM [7]. Still, optimization models that simultaneously balance MRR and *Ra* through intelligent decision-making remain scarce.

To address this gap, the current study proposes a comprehensive multi-objective optimization framework using NSGA-II combined with GPR as a surrogate model and the AHP for decision analysis. This combination leverages the search capability of evolutionary algorithms, the predictive accuracy of data-driven modeling, and the human-in-the-loop prioritization of performance metrics.

The need for multiple criteria optimizations in the presence of multiple interacting process variables and response parameters has been highlighted [8, 9]. In this context, the AHP enables the systematic ranking of solutions derived from Pareto fronts, thus facilitating practical decision-making for machining engineers. The importance of optimizing EDM process parameters to improve the machining performance in terms of both rate MRR and surface quality has been also stressed. A Multi-Criteria Decision-Making (MCDM) approach was employed to determine the optimal input parameters for the EDM of 90CrSi tool steel using graphite electrodes, revealing that pulse-on time, pulse-off time, peak current, and voltage significantly influence both MRR and *Ra* [10]. Likewise, investigations into the EDM of 7024 aluminum alloy have shown that discharge voltage and pulse-on time are critical factors in controlling the surface roughness and electrode wear, underscoring the need for precise parameter tuning [11]. Further research on Powder Mixed EDM (PM-EDM) of Ti-35Nb-7Zr-5Ta biomedical alloy has demonstrated that pulse energy density and powder concentration significantly affect surface characteristics and MRR [12]. Collectively, these findings highlight the necessity of employing multi-objective optimization strategies in EDM, particularly when addressing competing machining goals.

The present study contributes by developing a hybrid UV-EDM optimization framework that integrates NSGA-II, GPR, and the AHP, constructing a high-fidelity surrogate model based on experimental data, and identifying optimal machining parameters that effectively balance MRR and *Ra*. The work focuses on the machining of cylindrical surfaces made from 90CrSi steel, a material commonly used in the manufacturing of pharmaceutical tablet punches, sheet steel punches, and similar industrial components. Although UV-EDM has shown substantial promise in enhancing machining performance, there remains a strong demand for advanced, data-driven optimization strategies to fully exploit its capabilities. This study aims to address that need by contributing a novel, integrated methodology for efficient and high-quality machining in modern manufacturing environments.

II. METHODOLOGY

This work proposes an integrated approach to optimize UV-EDM, combining experimental design, statistical preprocessing, predictive modeling, and multi objective optimization techniques. The aim is to improve machining performance by increasing the MRR while reducing *Ra*, two goals that are often in conflict within the EDM process.

The methodology consists of five main stages:

1. Experimental design and data acquisition using Box-Behnken Design (BBD).
2. Data normalization via Box-Cox transformation.
3. Predictive modeling using GPR.
4. Multi-objective optimization through NSGA-II.
5. Decision-making using AHP.

A. Experimental Design Using Box-Behnken Design

The experimental dataset was generated using the BBD, a well-established response surface methodology that enables efficient estimation of second-order polynomial models without requiring test points at the corners of the design space [13]. BBD is particularly suitable for processes, like EDM,

where extreme parameter settings may lead to safety concerns or equipment damage due to high-energy discharges [14].

The input variables considered in this study were: ultrasonic vibration amplitude (*A,* in mm), pulse-on time (*Ton*, in µs), pulse-off time (*Toff*, in µs), peak current (*Ip*, in A), and gap voltage (*SV*, in V). The measured output responses included MRR in g/h, and *Ra* in µm. A total of 46 experimental runs were conducted based on the BBD matrix, staying well within the practical constraint of 50 tests, while still ensuring a statistically robust and safe exploration of the parameter space. BBD was chosen over Taguchi designs for its ability to capture both quadratic and interaction effects, and over Central Composite Design (CCD), which requires axial points at extreme parameter levels, conditions that are typically undesirable in EDM applications.

All experiments were carried out under controlled laboratory conditions, using the same electrode and workpiece materials throughout. Ultrasonic vibrations were applied longitudinally via a piezoelectric transducer operating at a frequency of 20kHz.

B. Data Transformation Using Box Cox Method

To improve the modeling performance and stabilize the variance of response variables, the experimental data were transformed using the Box-Cox transformation [15]. This transformation is particularly valuable in addressing heteroscedasticity and non-normality, which commonly arise in experimental data:

$$y^{(\lambda)} = \begin{cases} \frac{y^{\lambda}-1}{\lambda}, \lambda \neq 0 \\ ln(y), \lambda = 0 \end{cases} \quad (1)$$

where the original response (MRR or *Ra*) is transformed using a parameter λ, which is estimated through maximum likelihood. This transformation helps satisfy the assumptions of normality and constant variance (homoscedasticity), which are essential for reliable regression modeling.

C. Surrogate Modeling Using Gaussian Process Regression

Once transformed, the response data were used to develop surrogate models based on GPR, a non-parametric Bayesian regression technique well-suited for capturing nonlinear relationships in small to moderately sized datasets [16]. In GPR, the prediction at a new input point is represented as a Gaussian distribution, defined by a mean function *m(x)*, typically assumed to be zero and a covariance function or kernel *k(x,x')*, which captures the correlation between the input points.

This study employs the squared exponential kernel:

$$k(x,x') = \sigma_f^2 exp\left(-\frac{1}{2}(x-x')\Lambda^{-1}(x-x')\right) \quad (2)$$

where σ_f^2 is the signal variance, and Λ is a diagonal matrix of characteristic length-scales. The hyperparameters of the kernel were optimized using the marginal likelihood function. Cross-validation was used to evaluate the model accuracy and generalization capability. Model training was performed using MATLAB's GPR implementation with automatic hyperparameter tuning. A k-fold cross-validation technique was used to assess the model generalization performance.

D. Multi-Objective Optimization Using NSGA-II

The trained GPR models were embedded into a multi-objective optimization framework using the NSGA-II. The optimization problem was formulated as:

$$Maximized\ f_1(x) = MRR_{GPR}(x) \quad (3)$$

$$Minimized\ f_2(x) = Ra_{GPR}(x) \quad (4)$$

where *x* represents the input parameter vector. The NSGA-II is an evolutionary optimization algorithm known for its elite-preserving non-dominated sorting strategy and its use of crowding distance to maintain diversity in the solution set [17]. It is particularly effective for solving problems with conflicting objectives. In this study, NSGA-II was configured with a population size of 100, 150 generations, a crossover probability of 0.9, and a mutation probability of 0.1. The optimization process yields a Pareto front, representing the optimal trade-offs between high material removal and surface quality.

E. Application of AHP for Multi-Criteria Selection

To select the most appropriate solution from the Pareto-optimal set generated by the NSGA-II algorithm, the AHP was employed as a post-optimization decision-making tool. AHP is a widely deployed MCDM method that enables structured prioritization of alternatives through pairwise comparisons of evaluation criteria [18].

In this study, two conflicting criteria were considered: MRR, which should be maximized to enhance machining productivity, and Ra, which should be minimized to ensure surface quality. The decision-making process began with structuring the problem into a hierarchical model consisting of a single goal selecting the best machining solution, two criteria (MRR and *Ra*), and the set of Pareto optimal alternatives. A pairwise comparison matrix was then constructed using Saaty's fundamental 1–9 scale to express the relative importance between the two criteria. For instance, if MRR was judged moderately more important than Ra, a value of 3 was assigned to MRR with respect to *Ra*, and 1/3 to *Ra* with respect to MRR. The matrix was normalized, and the principal eigenvector was computed to derive the priority weights for the criteria.

To ensure the logical consistency of the judgments, the Consistency Ratio (CR) was calculated, with values below 0.1 considered acceptable. Each Pareto-optimal alternative was then normalized with respect to both criteria, benefit-type normalization for MRR and cost-type normalization for *Ra*. The final AHP score for each alternative was obtained as a weighted sum of the normalized values based on the derived weights. The alternative with the highest score from the AHP was selected as the most suitable solution. AHP proved to be a valuable tool for supporting clear and well-organized decision-making, helping to strike a balance between two key aspects of the process: productivity and surface integrity. By structuring the decision around what matters most to the user, the method ensured that the final choice reflected actual priorities, even when the latter are difficult to express numerically.

One of the strengths of AHP is its ability to break down complex decisions into smaller, more manageable parts. It considers both measurable data and more subjective factors, such as expert judgment or personal preferences. These are compared systematically, allowing each option to be evaluated fairly and consistently.

In summary, AHP offers a practical and adaptable framework for selecting between competing options, especially in cases where there are only a few key criteria but important trade-offs to consider. Its transparent process and focus on user-defined priorities make it an effective approach when decisions must be both rational and justifiable.

III. EXPERIMENTAL SETUP

An experiment was conducted to systematically investigate the influence of the main input process parameters UV-EDM. These parameters included the ultrasonic vibration amplitude (*A*), pulse-on time (*Ton*), pulse-off time (*Toff*), peak current (*Ip*), and gap voltage (*SV*). The goal was to assess their effect on two critical performance metrics: the MRR and the Ra of the machined workpiece. Figure 1 illustrates the experimental setup used in this study. The UV-EDM system was equipped with a copper electrode and used dielectric oil (Total Diel MS 7000) to promote stable discharge activity and effective debris flushing. The workpiece material was 90CrSi tool steel, selected for its high hardness and suitability in tool manufacturing applications. All experiments were carried out under controlled laboratory conditions to ensure repeatability. The experimental design matrix was constructed to cover a wide range of parameter settings while maintaining safe and realistic machining conditions. Table I presents the experimental input combinations along with the corresponding output results in terms of MRR and *SR*.

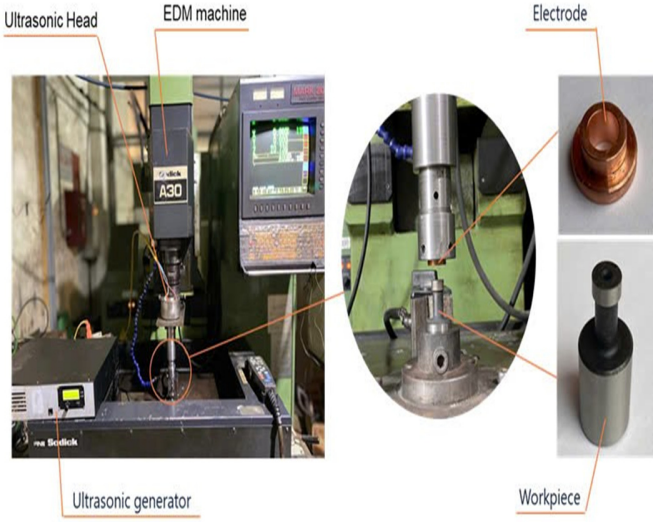

Fig. 1. Experimental setup.

TABLE I. PROCESS PARAMETERS AND EXPERIMENTAL RESULTS

Trial	*A* (mm)	T_{on} (µs)	T_{off} (µs)	*IP* (A)	*SV* (V)	*MRS* (g/h)	*Ra* (µm)
1	1.15	12	12	5	5	3.374	4.028
2	1.15	16	12	7	5	5.004	7.031
3	1.15	8	12	3	5	1.086	2.335
4	1.15	12	12	3	7	1.994	2.635
5	1.6	12	12	3	5	0.836	3.294
6	1.15	16	12	3	5	1.191	3.538
7	1.15	8	8	5	5	1.493	2.487
8	1.15	16	8	5	5	3.354	5.773
9	1.15	8	12	5	7	1.417	3.190
10	1.15	8	16	5	5	1.360	3.050
11	1.15	12	12	5	5	3.292	4.023
12	1.15	12	8	5	3	3.546	3.770
13	1.15	12	12	7	3	3.729	5.172
14	1.15	16	16	5	5	3.098	3.850
15	1.15	12	12	5	5	3.275	4.018
16	1.75	12	12	7	5	2.542	3.560
17	1.15	12	12	5	5	3.249	4.015
18	1.15	12	8	5	7	3.349	3.550
19	1.6	16	12	5	5	1.972	3.555
20	1.6	12	8	5	5	2.506	3.580
21	1.75	12	12	5	7	1.669	3.610
22	1.15	8	12	7	5	1.392	3.190
23	1.75	8	12	5	5	0.305	2.687
24	1.6	12	16	5	5	2.373	3.760
25	1.15	12	8	7	5	4.054	5.200
26	1.15	12	16	5	3	3.252	3.755
27	1.15	12	12	5	5	3.313	4.026
28	1.15	12	8	3	5	1.996	3.787
29	1.15	16	12	5	3	2.947	3.530
30	1.15	16	12	5	7	3.517	3.780
31	1.15	12	16	7	5	3.736	4.720
32	1.15	12	16	5	7	3.202	4.770
33	1.75	12	16	5	5	2.156	4.790
34	1.15	12	12	7	7	3.609	4.710
35	1.75	12	8	5	5	2.322	4.300
36	1.6	12	12	7	5	2.720	4.441
37	1.15	8	12	5	3	1.349	3.010
38	1.15	12	12	5	5	3.390	4.031
39	1.6	12	12	5	7	2.210	4.740
40	1.75	16	12	5	5	1.828	3.540
41	1.6	8	12	5	5	0.361	2.675
42	1.6	12	12	5	3	2.372	4.210
43	1.15	12	12	3	3	1.275	3.161
44	1.75	12	12	3	5	0.916	3.785
45	1.15	12	16	3	5	1.914	3.685
46	1.75	12	12	5	3	2.034	4.116

IV. RESULTS AND DISCUSSION

A. NSGA-II Pareto Optimization using GPR Surrogate

The GPR model, enhanced with Box–Cox transformation, exhibited strong predictive performance across the entire design space of EDM parameters. This surrogate model accurately estimated both the MRR and *Ra*, significantly reducing the number of required physical experiments. Based on the predictions of this model, the NSGA-II algorithm successfully generated a diverse set of Pareto-optimal solutions that reflect the inherent trade-off between productivity and surface quality in the EDM process.

In industrial applications , particularly in the manufacturing of tablet punch tools, EDM is often used as a semi finishing process. In this context, the present study specifies that the Ra of the machined workpieces must not exceed Ra=4 µm to meet the quality standards.

Figure 2 illustrates the tradeoff surface produced by the NSGA-II optimization. The Pareto front ranges from solutions that yield high MRR but poor surface quality, to those offering excellent surface finish at the expense of reduced material removal. At one end of the spectrum, an aggressive parameter setting achieves an MRR of approximately 5.0 g/h with *Ra* around 7.0 µm, clearly violating the *Ra* constraint. Conversely, a more conservative configuration results in Ra approximately 2.3 µm but limits MRR to about 1.2 g/h. These two extremes underscore the fundamental trade-off in EDM: increasing discharge energy via I*p* or *Ton,* improving material removal but degrading surface quality due to deeper crater formation and more intense thermal stress.

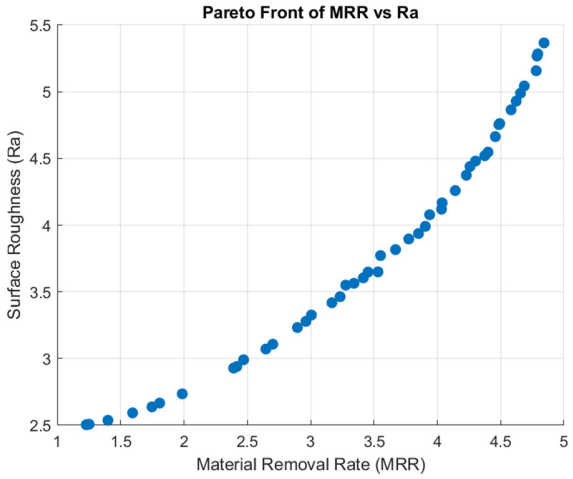

Fig. 2. Pareto Front of MRR and *Ra*.

This behavior is consistent with the findings reported in earlier EDM studies, where the peak current was identified as the most influential factor affecting both MRR and *Ra* [19]. A higher current leads to an increased spark energy, which accelerates the material erosion but also causes unstable crater morphology and thicker recast layers. While such aggressive parameters may be desirable in roughing operations, they are unsuitable in semi-finishing contexts, like tablet punch production, where Ra must be strictly controlled. By visualizing the Pareto front, manufacturers and process engineers can observe the performance boundary and identify regions that maximize MRR while remaining within acceptable quality limits (*Ra*≤4 µm). This capability provides a practical and efficient way to tailor EDM parameters to the specific demands of die or punch tool fabrication.

B. Trade-off Analysis of Pareto Solutions

The set of Pareto-optimal solutions generated by NSGA-II reveals a diverse range of trade-offs between MRR and *Ra*. However, in practical applications, such as semi-finishing EDM, for tablet punch manufacturing, not all Pareto-optimal solutions are viable. Only those configurations that satisfy the surface roughness constraint of Ra≤4 µm are considered acceptable. This threshold reflects real-world quality requirements and serves as a practical boundary for selecting suitable process parameters. Even within this constrained region, the Pareto front continues to display significant variation in both MRR and *Ra*. As displayed in Figure 2, feasible MRR values range from approximately 1.3 to 3.8 g/h, while corresponding Ra values vary from around 2.3 to 4.0 µm.

1) High-MRR Feasible Solution

This solution delivers an MRR of approximately 3.77 g/h with Ra approximately to 4.0 µm, exactly at the threshold of Ra tolerance. It is characterized by moderately high peak current and relatively long pulse-on time, which promote high material removal while carefully avoiding excessive surface damage. This solution represents the upper limit of productivity that still satisfies the surface quality requirements. In real production settings, such a solution is highly desirable, as it maximizes the throughput without violating quality specifications.

2) Surface-Focused Solution

On the opposite end of the feasible region, some solutions achieve Ra values between 2.3 and 2.5 µm, but with much lower MRR ranging from 1.3 to 1.5 g/h. These solutions result from applying lower discharge energy, such as reduced peak current and shorter pulse-on durations, to prioritize surface integrity. While such settings may be useful in applications where surface finish is critical (e.g., fine-feature EDM or mold inserts), they are suboptimal for tablet punch production, where $Ra \leq 4$ µm is sufficient and higher productivity is preferred.

3) Balanced Feasible Solutions

Between the two extremes lies a range of compromise solutions that achieve moderately high MRR values between 2.8 and 3.5 g/h and Ra values between 3.2 and 3.8 µm, all remaining safely below the 4 µm threshold. These represent attractive operating points for industrial EDM processes that seek to balance the surface quality with machining efficiency. In this study, such points were further evaluated using AHP to identify which specific settings best align with the manufacturer's productivity and quality priorities. The trend observed on the Pareto front illustrates the fundamental trade-off between maximizing material removal and maintaining surface quality. Increasing discharge energy, typically by raising the peak current or extending the pulse-on time, results in higher MRR because more material is removed with each spark. However, this also intensifies the thermal and plasma effects, which tend to degrade the machined surface and increase *Ra*. This creates a practical limit in process performance, and multi-objective optimization helps identify the best possible operating conditions without exceeding constraints, such as $Ra \leq 4$ µm.

In tablet punch manufacturing, the most favorable solutions are those that achieve the highest possible MRR while keeping *Ra* just below the acceptable threshold of 4 µm. These settings allow manufacturers to operate close to maximum machining efficiency, while still meeting the surface finish requirements needed for subsequent processes, such as polishing or coating.

C. Multi-Criteria Decision Analysis with AHP

To select the most appropriate solution among the Pareto-optimal points that meet the constraints of $Ra \leq 4\mu m$ and MRR> 3 g/min, AHP was applied. This MCDM method enables a structured evaluation of alternatives based on multiple criteria, in this case MRR and *Ra*, by assigning preference weights to each. The weight assigned to MRR is denoted as *wMRR*, while the corresponding weight for Ra is expressed as (1−*wMRR*). To demonstrate how varying the priority given to MRR influences the optimal solution identified by AHP, Figure 3 shows the change in the highest AHP score as *wMRR* varies from 0 to 1.

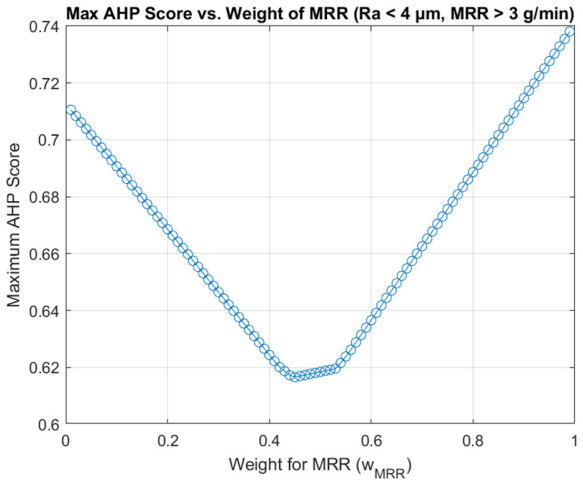

Fig. 3. Effect of MRR weight on the maximum AHP score for feasible Pareto solutions.

Figure 3 represents how the highest AHP score among the feasible Pareto solutions varies as the weight assigned to MRR (*wMRR*) changes from 0 to 1. The resulting curve forms a clear V shape, offering valuable insight into how different decision-making priorities influence the outcome.

When *wMRR* is around 0.45 to 0.55, meaning that MRR and Ra are given approximately equal importance, the highest AHP scores remain relatively low, typically between 0.615 and 0.620. This indicates that no solution performs significantly better than the others under equal weighting. In such cases, the selected solutions tend to offer moderate values for both MRR and *Ra*, and thus do not stand out in the ranking.

As the preference shifts more strongly toward MRR, with *wMRR* greater than 0.6, the AHP scores rise sharply. The peak score reaches approximately 0.74 when *wMRR* approaches 1. This suggests that when productivity is prioritized, the optimal solution corresponds to the highest MRR that still meets the requirement of Ra less than or equal to 4 µm. In contrast, when surface quality is prioritized and *wMRR* falls below 0.4, the scores also increase slightly but never reach the same levels. This is because the solutions with the lowest Ra tend to significantly reduce MRR, and since the actual constraint is to keep Ra below 4 µm not to minimize it entirely. Those options are less favorable from a manufacturing perspective.

This analysis shows that the highest-ranked solution according to AHP is obtained when MRR is assigned a high weight. In this case, the algorithm consistently selects the setting that achieves the greatest feasible MRR while still complying with the surface finish limit. In the present study, this solution yields an MRR of about 3.77 g/min and a Ra close to 4.0 µm. Observing how the best AHP score responds to changes in *wMRR* provides a useful guide for decision makers, especially when production goals or quality standards vary over time.

D. Role of Ultrasonic Vibration in Performance Improvement

This study demonstrated that incorporating ultrasonic vibration into the EDM process leads to a clear improvement in the material removal performance. The enhanced version of the process, known as UV-EDM, was compared with conventional EDM under optimized conditions for each case. For the conventional setup, using the manufacturer's recommended parameters (*Ton* = 10 µs, *Toff* =10 µs, *Ip* =4 A, *SV*=5 V), the MRR reached 1.492 g/h with a Ra of 2.872 µm. In contrast, the optimal settings identified for UV-EDM through multi-criteria decision analysis based on the AHP were *Ton*=12 µs, *Toff*=11 µs, *Ip* =5 A, and *SV* =5 V. Under these conditions, MRR increased to 3.77 g/h, while *Ra* remained within acceptable limits at 4.0 µm. This corresponds to an increase of more than 150% in the material removal rate, achieved without exceeding the *Ra* threshold.

This improvement is primarily attributed to a more effective evacuation of debris from the inter-electrode gap. The high-frequency vibration promotes stable discharge activity and reduces spark interruptions, allowing more of the electrical energy to be utilized for material removal and improving overall machining efficiency. Similar observations have been reported during the EDM of SiCp/Al composites, where ultrasonic vibration led to both higher MRR and lower *Ra*, highlighting the importance of tuning vibration parameters for optimal performance [20].

Overall, the integration of ultrasonic vibration makes it possible to apply more aggressive discharge energy settings while maintaining surface finish within acceptable limits. This results in a substantial increase in machining productivity and makes UV-EDM a highly suitable option for semi-finishing operations, such as those used in die and punch manufacturing.

E. Novelty and Contribution Compared to Previous Research

Previous research on UV-EDM has primarily focused on internal geometries, such as micro-holes, slots, and enclosed grooves [4]. While these studies have demonstrated improvements in discharge stability and surface quality, their findings are largely limited to applications involving internal features.

In contrast, the present study investigates the feasibility of UV-EDM for machining external cylindrical surfaces, a geometry commonly encountered in tablet punch tools and similar industrial components. Figure 4 portrays representative workpieces used in this study, highlighting the type of external surfaces addressed. The ability to apply UV-EDM to such geometries expands the process beyond traditional limitations.

This is enabled by a custom ultrasonic horn that delivers vibration directly to the electrode, allowing energy transmission without modifying the workpiece. As a result, the system can accommodate different cylindrical geometries without requiring vibration customization for each case.

In addition, the study introduces an integrated optimization framework combining GPR for predictive modeling, NSGA-II for parameter exploration, and the entropy-weighted MABAC method for final decision-making. This approach supports both theoretical insights and practical applications in semi finishing EDM processes involving challenging geometries.

Fig. 4. Tablet punch components with external cylindrical geometry.

V. CONCLUSION

This study proposed a complete optimization methodology for Ultrasonic Vibration-Assisted Electrical Discharge Machining (UV-EDM), focusing on semi-finishing operations in the manufacturing of hardened 90CrSi steel tablet punch tools. The approach integrates data-driven modeling, evolutionary optimization, and structured decision analysis to identify the machining parameters that maximize material removal while satisfying Ra constraints.

The findings demonstrated that UV-EDM significantly enhances productivity without compromising surface quality, particularly when vibration is applied directly to the electrode. The developed framework, based on Gaussian Process Regression (GPR), Non-Dominated Sorting Genetic Algorithm II (NSGA-II), and Analytic Hierarchy Process (AHP), offers a systematic and interpretable tool for process parameter selection under realistic industrial conditions.

Future work may involve the inclusion of additional performance criteria, such as tool wear or dimensional accuracy, or the development of adaptive, real-time optimization systems for intelligent Electrical Discharge Machining (EDM) control.

ACKNOWLEDGMENT

The authors gratefully acknowledge the support provided by Thai Nguyen University of Technology (TNUT) for this research.

REFERENCES

[1] A. Hirao, H. Gotoh, and T. Tani, "Some Effects on EDM Characteristics by Assisted Ultrasonic Vibration of the Tool Electrode,"*Procedia CIRP*, vol. 68, pp. 76–80, Jan. 2018, https://doi.org/10.1016/j.procir.2017.12.025.

[2] J. Singh, R. Walia, P. Satsangi, and V. Singh, "FEM modeling of ultrasonic vibration assisted work-piece in EDM process," *International Journal of Mechanic Systems Engineering*, vol. 1, no. 1, pp. 8–16, Jan, 2011.

[3] P. Zhang *et al.*, "Investigating mechanisms of debris removal in ultrasonic vibration-assisted EDM drilling," *International Journal of Mechanical Sciences*, vol. 279, Oct. 2024, , Art. no. 109486, https://doi.org/10.1016/j.ijmecsci.2024.109486.

[4] Z. Yin *et al.*, "A novel EDM method using longitudinal-torsional ultrasonic vibration (LTV) electrodes to improve machining performance for micro-holes," *Journal of Manufacturing Processes*, vol. 102, pp. 231–243, Sep. 2023, https://doi.org/10.1016/j.jmapro.2023.07.023.

[5] J. Tang, Z. Li, and J. Bai, "Investigation of depth error of microgroove in micro-EDM adopting ultrasonic circular vibration (UCV) electrode," *The International Journal of Advanced Manufacturing Technology*, vol. 131, no. 7, pp. 4009–4020, Apr. 2024, https://doi.org/10.1007/s00170-024-13283-7.

[6] Y. Wang, L. Fan, J. Shi, Y. Dong, and Z. Fu, "Effect of cavitation on surface formation mechanism of ultrasonic vibration-assisted EDM," *The International Journal of Advanced Manufacturing Technology*, vol. 124, no. 10, pp. 3645–3656, Feb. 2023, https://doi.org/10.1007/s00170-022-10780-5.

[7] M. R. Shabgard, A. Gholipoor, and M. Mohammadpourfard, "Numerical and experimental study of the effects of ultrasonic vibrations of tool on machining characteristics of EDM process," *The International Journal of Advanced Manufacturing Technology*, vol. 96, no. 5, pp. 2657–2669, May 2018, https://doi.org/10.1007/s00170-017-1487-3.

[8] C. Praneetpongrung, Y. Fukuzawa, S. Nagasawa, and K. Yamashita, "Effects of the Edm Combined Ultrasonic Vibration on the Machining Properties of Si3N4," *Materials Transactions*, vol. 51, no. 11, pp. 2113–2120, Nov. 2010, https://doi.org/10.2320/matertrans.M2010194.

[9] Y.-C. Lin, J.-C. Hung, H.-M. Chow, A.-C. Wang, and J.-T. Chen, "Machining Characteristics of a Hybrid Process of EDM in Gas Combined with Ultrasonic Vibration and AJM," *Procedia CIRP*, vol. 42, pp. 167–172, Jan. 2016, https://doi.org/10.1016/j.procir.2016.02.213.

[10] T. P. T. Le, V. T. Dinh, T. Q. D. Nguyen, D. B. Vu, and T. T. Vu, "Application of the Multi-Criteria Decision Method to Find the Best Input Factors for Electrical Discharge Machining 90CrSi Tool Steel using Graphite Electrodes," *Engineering, Technology & Applied Science Research*, vol. 14, no. 6, pp. 18883–18888, Dec. 2024, https://doi.org/10.48084/etasr.9114.

[11] S. K. Ghazi, M. A. Abdullah, and H. H. Abdulridha, "Investigating the Impact of EDM Parameters on Surface Roughness and Electrode Wear Rate in 7024 Aluminum Alloy," *Engineering, Technology & Applied Science Research*, vol. 15, no. 1, pp. 19401–19407, Feb. 2025, https://doi.org/10.48084/etasr.9252.

[12] A. R. Hayyawi, H. Al-Ethari, and A. H. Haleem, "Optimization of the PM-EDM Process Parameters for Ti-35Nb-7Zr-5Ta Bio Alloy," *Engineering, Technology & Applied Science Research*, vol. 14, no. 3, pp. 13982–13989, Jun. 2024, https://doi.org/10.48084/etasr.6845.

[13] G. E. P. Box and D. W. and Behnken, "Some New Three Level Designs for the Study of Quantitative Variables," *Technometrics*, vol. 2, no. 4, pp. 455–475, Nov. 1960, https://doi.org/10.1080/00401706.1960.10489912.

[14] J. Lei, H. Shen, H. Wu, W. Pan, X. Wu, and C. Zhao, "Ultrasonic vibration-assisted electrical discharge machining of enclosed microgrooves with laminated electrodes," *Journal of Materials Research and Technology*, vol. 30, pp. 9521–9530, May 2024, https://doi.org/10.1016/j.jmrt.2024.06.035.

[15] G. E. P. Box and D. R. Cox, "An Analysis of Transformations," *Journal of the Royal Statistical Society Series B: Statistical Methodology*, vol.

26, no. 2, pp. 211–243, Jul. 1964, https://doi.org/10.1111/j.2517-6161.1964.tb00553.x.

[16] C. E. Rasmussen and C. K. I. Williams, *Gaussian Processes for Machine Learning*, 1st ed. Cambridge, MA, USA: MIT Press, 2005.

[17] K. Deb, A. Pratap, S. Agarwal, and T. Meyarivan, "A fast and elitist multiobjective genetic algorithm: NSGA-II," *IEEE Transactions on Evolutionary Computation*, vol. 6, no. 2, pp. 182–197, Apr. 2002, https://doi.org/10.1109/4235.996017.

[18] T. L. Saaty, *Decision Making with Dependence and Feedback: The Analytic Network Process : the Organization and Prioritization of Complexity*, 2nd ed. Maidenhead, Berkshire, UK: RWS Publications, 1996.

[19] M. K. Das, K. Kumar, T. Kr. Barman, and P. Sahoo, "Application of Artificial Bee Colony Algorithm for Optimization of MRR and Surface Roughness in EDM of EN31 Tool Steel," *Procedia Materials Science*, vol. 6, pp. 741–751, Jan. 2014, https://doi.org/10.1016/j.mspro.2014.07.090.

[20] X. Gao, J. Li, Q. Xing, and Q. Zhang, "Research on ultrasonic vibration–assisted electrical discharge machining SiCp/Al composite," *The International Journal of Advanced Manufacturing Technology*, vol. 121, no. 3, pp. 2095–2113, Jul. 2022, https://doi.org/10.1007/s00170-022-09352-4.